Orbital Magnetic Dipole Mode in Deformed Clusters: A Fully Microscopic Analysis

V. O. Nesterenko,[1,2] W. Kleinig,[2,3] F. F. de Souza Cruz,[1] and N. Lo Iudice[4]
[1]*Departamento de Fisica, Universidade Federal de Santa Catarina, 88040-900, Florianopolis, SC, Brasil*
[2]*Bogoliubov Laboratory of Theoretical Physics, Joint Institute for Nuclear Research, 141980 Dubna, Moscow region, Russia*
[3]*Technische Universität Dresden, Institut für Analysis, D-01062 Dresden, Germany*
[4]*Università di Napoli "Federico II" and Istituto Nazionale di Fisica Nucleare, Dipartamento di Scienze Fisiche, Monte S. Angelo, Via Cintia I-80126, Napoli, Italy*
(Received 11 February 1999; revised received date 7 June 1999)

The orbital $M1$ collective mode predicted for deformed clusters in a schematic model is studied in a self-consistent random-phase-approximation approach which fully exploits the shell structure of the clusters. The microscopic mechanism of the excitation is clarified and the close correlation with the $E2$ mode established. The study shows that the $M1$ strength of the mode is fragmented over a large energy interval. In spite of that, the fraction remaining at low energy, well below the overwhelming dipole plasmon resonance, is comparable to the strength predicted in the schematic model. The importance of this result in view of future experiments is stressed.

PACS numbers: 36.40.Cg, 36.40.Gk, 36.40.Vz, 36.40.Wa

Among the collective excitations which may occur in metal clusters, the magnetic dipole mode predicted for deformed clusters in a schematic model [1] has unique and appealing properties which deserve a deeper investigation. This excitation, which is the analog of the scissors mode predicted [2] and observed [3] in deformed nuclei, is promoted by rotational oscillations of the valence electrons against the jellium background. Indeed, in the semiclassical approach [1], the displacement field of the mode is composed of a rigid rotational velocity field plus a quadrupole term which comes from the boundary condition that the velocity flow vanishes on the deformed surface. The distortion of the momentum Fermi sphere generates a restoring force of the rotational oscillations. The mode is characterized by the magnetic quantum number $K^\pi = 1^+$ and falls at an excitation energy [1]

$$\omega_{M1} = \sqrt{2}\,\omega_0\delta\,\frac{1}{\sqrt{1 + 5\omega_0^2/\omega_p^2}} \simeq \frac{20.7}{r_s^2}\,N_e^{-1/3}\delta \text{ eV}, \tag{1}$$

where $\omega_0 = (2\epsilon_F/mr_s^2)^{1/2}N_e^{-1/3}$ and ω_p are, respectively, the harmonic oscillator (HO) and the plasma frequencies; δ is the deformation parameter, r_s is the Wigner-Seitz radius, ϵ_F is the Fermi energy ($r_s = 2.1$ Å and $\epsilon_F = 3.1$ eV for Na clusters), and N_e is the number of valence electrons in a cluster. The latter is related to the number N of atoms in a cluster by $N = N_e$ or $N = N_e + 1$ according to the fact that the cluster is neutral or has a positive charge $Z = +1$. The mode gets a $M1$ strength given by

$$B(M1) = 2|\langle K^\pi = 1^+|\sum_i l_x(i)|0\rangle|^2\mu_b^2 = \Im\omega_{M1}\mu_b^2 \simeq N_e^{4/3}\delta\,\mu_b^2\,, \tag{2}$$

where $\Im = 2/3\,N_e m\langle r^2\rangle = 2/5 r_s^2 m N_e^{5/3}$ is the collective mass parameter. As the formulas show, the $M1$ mode is peculiar of deformed clusters. Its occurrence would represent a unique and unambiguous fingerprint for the onset of quadrupole deformation. The main indicator of the deformation available so far is the splitting of the $E1$ resonance which, however, is often washed out or not properly resolved experimentally. The energy formula (1) reveals another appealing property. The $M1$ mode falls well below the energy of the overwhelming $E1$ resonance and, therefore, has good chances of being detected experimentally. In view of such a possibility, it is of the utmost importance to test the predictions of the schematic model by carrying out a microscopic calculation which fully exploits the shell structure of the clusters. Such a calculation should shed light on the microscopic mechanism which generates the mode and should reveal, eventually, new properties connected with the shell structure. It certainly will ascertain if and to what extent the $M1$ strength is fragmented and quenched. Clearly such a mode can be detected and can be used as a signature for deformation only if its $M1$ strength remains concentrated in a reasonably narrow energy range.

We performed our calculation in a self-consistent random-phase-approximation (SRPA) approach [4–6] which in the most general formulation [4] is based on the Kohn-Sham functional [7]. Here we skipped the self-consistent derivation of the one-body potential and adopted the phenomenological deformed Woods-Saxon well. On the other hand, we determined self-consistently the two-body potential starting with a set of displacement fields ∇f_{L21}, where

$$f_{L21} = r^L(Y_{21} + Y_{21}^*), \qquad L = 2, 4, 6, 8. \tag{3}$$

The resulting interaction was a sum of weighted separable terms peaked on different slices of the system. Because of its close link to the detailed structure of the system, such an interaction, in spite of its separable form, came out to be quite suitable for describing its dynamical properties. The SRPA fully exploits the shell structure and, as shown

 © 1999 The American Physical Society

for the dipole response [6], reaches the accuracy of the most refined and complete RPA approaches. Moreover, it preserves the simplicity of the schematic model [1] which can be easily recovered if an anisotropic HO potential plus the single operator $f_{221} = r^2(Y_{21} + Y_{21}^*)$ is used.

The choice of a quadrupolelike field was motivated by its close connection with the generator of the rotational oscillation, namely, the angular momentum (see [8], and references therein). Such a link can be easily established for $L = 2$ in the HO space, where one finds

$$\langle p|l_x|h\rangle \simeq \sqrt{\frac{4\pi}{15}}\, mb(\omega_0)\langle p|f_{221}|h\rangle \qquad (4)$$

being $b(\omega_0) = 2\omega_0$ for the $\Delta\mathcal{N} = 0$ space and $b(\omega_0) = \delta\omega_0$ for $\Delta\mathcal{N} = 2$ ($\mathcal{N}$ is a principle shell quantum number). On the other hand, the quadrupole fields act obviously also in the $E2$ channel. Consistency requires that both, magnetic dipole and electric quadrupole, excitations should be treated contextually. It is worth noting that, the choice made for our displacement fields [see Eq. (3)] is quite general for our purposes. Indeed, since spin-orbit coupling in clusters is negligible, the orbital excitations are decoupled from the spin ones, so that the spin-spin interaction can be safely neglected. The spin-quadrupole fields can be also ignored. In the nuclear systems, they are known to affect only the spin channel by renormalizing the spin-spin interaction.

The parameters of the Woods-Saxon potential $V_{WS} = V_0/\{1 + \exp[(R(\Theta) - r)/a_0]\}$ with $R(\Theta) = R_0[\beta_0 + \beta_2 Y_{20}(\Theta)]$ and $R_0 = r_0 N^{1/3}$ were adjusted so as to reproduce the Kohn-Sham + SRPA results for the dipole plasmon in spherical sodium clusters [4]. The fit yielded $r_0 = 2.5$ Å, $V_0 = -7.2$ eV, and $a_0 = 1.25$ Å for singly charged clusters and $r_0 = 2.4$ Å, $V_0 = -5.7$ eV, and $a_0 = 1.11$ Å for neutral clusters. The values of the deformation parameter $\delta = \sqrt{45/16\pi}\,\beta_2$ were extracted from the experimental data [9] (for $N_e \leq 34$) following the prescription of Ref. [1], or were taken from the calculations [10] (for $N_e > 34$). Only clusters with measured or predicted *axial* quadrupole deformation were considered. Equal deformation parameters were used for both charged and neutral clusters. As shown in Ref. [5], the SRPA calculations with these parameters account well for the observed deformation splitting of the dipole plasmon in deformed Na clusters.

The most meaningful results of the calculation are presented in Figs. 1–3. In Fig. 1 the $M1$ strength distribution is plotted for singly charged clusters varying from $N = 15$ to 295. In order to simulate the temperature broadening, we smoothed out the $M1$ strength with the Lorentz weight using the averaging parameter $\Delta = 0.05$ eV. Such a simulation is in general rather rough as compared to an explicit treatment of electronic and ionic thermal fluctuations. Nonetheless, since we do not pretend to describe specific thermal effects, this simulation should be sufficient for our purposes, if we confine ourselves within the temperature interval 300–600 K, where jellium approximation is appropriate. We also gave in Fig. 1 a quantitative estimate of the Landau damping by computing the width Γ of the resonance which ideally envelops all the peaks above a threshold value fixed to be one-half the height of the highest

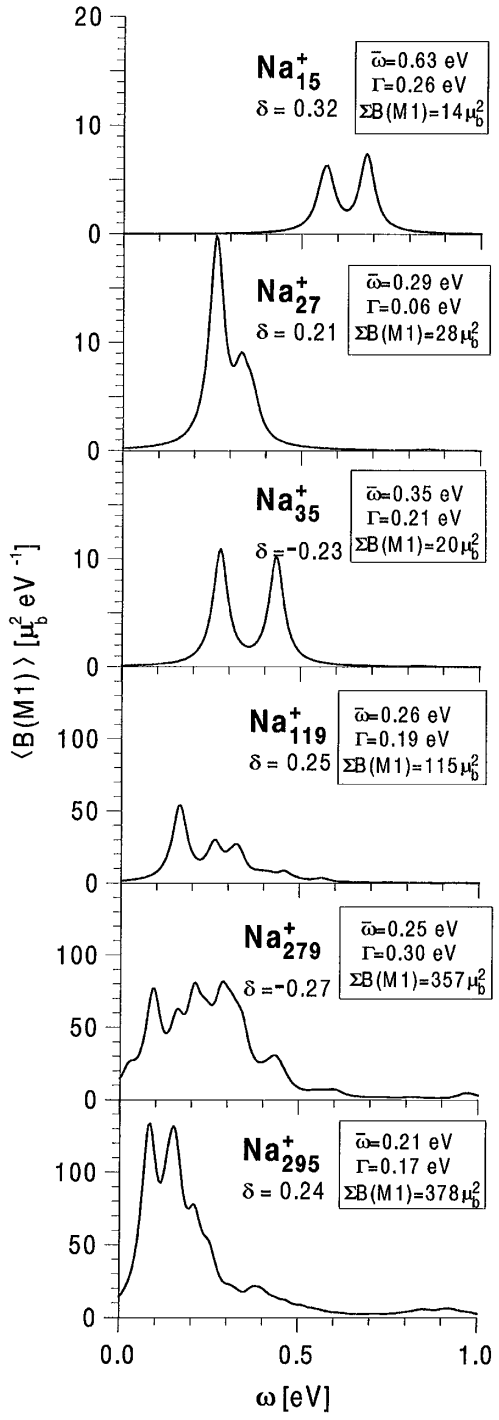

FIG. 1. Energy distribution of the $M1$ strength over the interval 0–1 eV for sodium clusters ranging from $N = 15$ to 295. The deformation parameter δ, the energy centroid $\overline{\omega}$, the quantity Γ for estimating the Landau damping, and the summed $M1$ strength [$\sum B(M1)$] are given for each cluster.

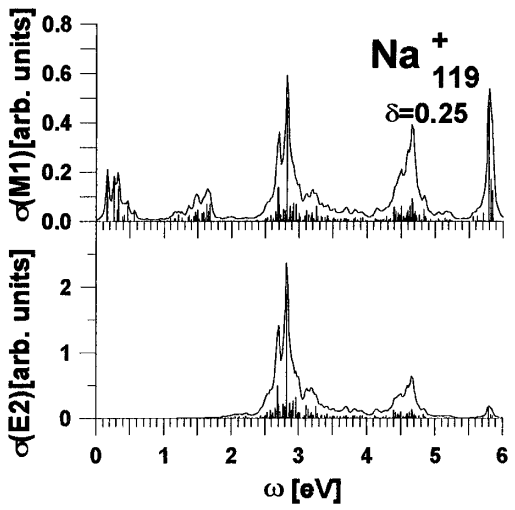

FIG. 2. Plot of the $M1$ and $E2$ SRPA photoabsorption cross sections over the full energy range in Na_{119}^{+}. The curves give the Lorentz averaged SRPA response, while the underlying bars show the pure discrete spectra, which better illustrate the Landau damping.

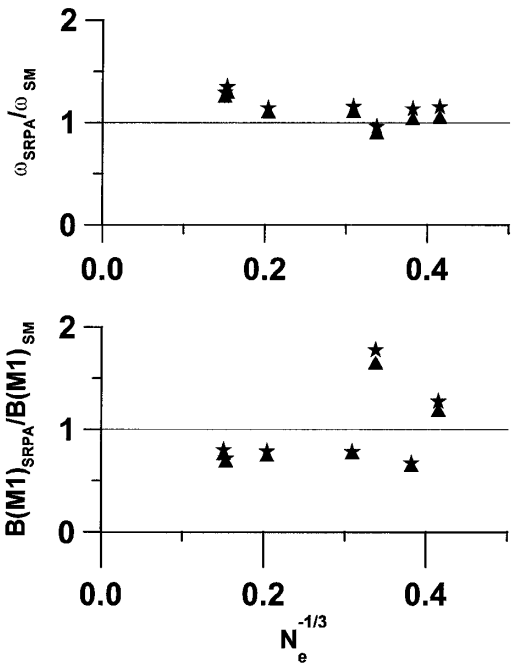

FIG. 3. Ratios between SRPA energy centroids (top) and $M1$ strengths (bottom), summed over 0–1 eV, and the corresponding schematic estimates [Eqs. (1) and (2)] for charged (stars) and neutral (triangles) clusters with N_e =14, 18, 26, 34, 118, 278, and 294.

peak [6]. This definition yields the standard full width at half maximum (FWHM) in the simplest case of one-peak structure. The plot shows that, as the size of the cluster increases, the whole $M1$ strength is shifted downward with rising magnitude and fragmentation. Only in going from the light prolate Na_{27}^{+} to the light oblate Na_{35}^{+}, this trend is not observed. In heavy clusters with $N_e \sim 300$, the $M1$ strength reaches the huge values $(350-400)\mu_b^2$. The fragmentation (Landau damping) gets also very pronounced, since Γ and $\overline{\omega}$ become comparable. Because of the small value of $\overline{\omega}$, however, the strength remains concentrated in a rather narrow energy interval.

The softening of the mode as well as the enhancement of the $M1$ strength can be nicely explained within the semiclassical model with the decreasing importance of the surface with respect to the bulk as the sizes of the cluster increase. This causes a faster increase of the mass parameter with respect to the restoring force constant coming almost entirely from a surface shear, with consequent lowering of the energy centroid (1) and enhancement of the $M1$ strength (2). A more detailed and exhaustive explanation is provided by the microscopic excitation mechanism. By expanding the deformed single-particle wave function into a spherical basis $|m\rangle = \sum_{nl} a_{nl}^{m} |nlm\rangle$ and accounting for the fact that each $|m\rangle$ state is, in general, dominated by a single spherical configuration $|nlm\rangle$, one obtains the transition amplitude

$$\langle m'|\hat{l}_{\pm}|m\rangle \simeq \mp\delta_{m',m\pm1}\sqrt{l(l+1) - m(m\pm1)}\,. \quad (5)$$

Clearly, the main contribution to the transition amplitude comes from orbits with high angular momentum l and small magnetic quantum number m. On the other hand, orbits with high l values are present only in heavy clusters, hence the enhancement of the $M1$ strength. At the same time, as the sizes of the cluster increase with consequent increment of the number of high values of l, the density of the particle-hole $(p\text{-}h)$ levels increases and their relative spacings decrease, causing an overall downward shift and a more pronounced fragmentation of the $M1$ strength. The above formula enables one to sharpen the geometrical picture of the mode. Since most of the strength comes from orbits with high l and small m values, it follows that the oscillatory rotational motion is promoted mainly by the orbits which are almost orthogonal to the equatorial plane.

In light clusters the $M1$ transition is promoted mainly by one or two configurations. Indeed, the left and right peaks are due by more than 95% to the $p\text{-}h$ components [200]-[211] and [202]-[211] in Na_{15}^{+}, [312]-[321] and [310]-[321] in Na_{27}^{+}, and [321]-[310] and [321]-[312] in Na_{35}^{+}, having adopted the Nilsson-Clemenger notation $Nn_z\Lambda$ [11] for the single-particle orbitals. The reason for the small $p\text{-}h$ admixture induced by the residual interaction is simple. The $p\text{-}h$ configurations are very few and far apart in energy. The only observable effect of the interaction is therefore a shift of the $M1$ strength. We may therefore conclude that in light nuclei the $M1$ mode has the character of a single-particle excitation. Only in heavy clusters does the collective nature of the mode appear evident.

Figure 2 shows the $M1$ and $E2$ responses of Na_{119}^{+} over a much wider energy interval. For a more homogeneous comparison, we give the photoabsorption cross sections,

$\sigma(M1, \mu = 1) \sim \sum B(M1, \mu = 1)\omega$ and $\sigma(E2, \mu = 1) \sim \sum B(E2, \mu = 1)\omega^3$, rather than the strengths. The $M1$ spectrum is composed of several, roughly equally spaced, resonances, enveloping closely packed transitions, coming, respectively, from $\Delta\mathcal{N} = 0, 2, 4, \ldots,$ p-h excitations. The group of $\Delta\mathcal{N} = 0$ transitions correspond to the low-lying $M1$ mode predicted in the schematic model [1]. The others have no classical counterpart. This large scale fragmentation drastically limits the extent of validity of approaches which rely entirely on sum rules. It is worth noting, on the other hand, that the cross section, being proportional to the energy weighted $M1$ strength, magnifies the high-energy transitions. Had we plotted the $M1$ strength, we would have observed a most prominent peak positioned in the lowest-energy region and several others, much less pronounced, at higher energy. It is also to be pointed out that the high-energy peaks which are physically relevant, namely, the ones below the ionization threshold (which is 3.8 eV in light clusters and 3.2–3.4 eV in the heavier ones), overlap mostly with the dipole plasmon resonance and, therefore, are hardly detectable.

The lower panel of Fig. 2 shows that, consistent with the HO relation (4), the $E2$ strength covers the same energy regions of the $M1$ strength. It is, however, dominant over the $M1$ transition only in the intermediate region, which is in any case the domain of the dipole plasmon resonance, and almost absent in the low-energy region. This latter interval is *exclusively* covered by the $M1$ mode, consistent with the predictions of the schematic model.

A more quantitative comparison with this model is presented for the low-energy mode in Fig. 3. Although the schematic Eqs. (1) and (2) were derived for neutral clusters only, we considered both charged and neutral clusters. Indeed, the results change very little in moving from one kind to the other. The energy centroids of the low-energy $M1$ transitions scale with deformation and the number of valence electrons basically according to the law derived in the schematic model [1]. The summed $M1$ strength scales according to the schematic law only in heavy clusters, but fluctuates strongly in the light ones. These fluctuations reflect the single-particle nature of the transitions and, in principle, invalidate the schematic model for clusters of these sizes. The low-lying $M1$ strength is of order of the semiclassical estimates and even larger in light clusters. Moreover, this strength summed in the interval 1–6 eV exceeds systematically (up to 10%–100%) the estimate (2). This looks surprising since in the schematic model the mode gets the total $M1$ strength by construction. This apparent paradox is solved if we recall that the semiclassical calculation of the strength is fully equivalent to its RPA evaluation in the $\Delta\mathcal{N} = 0$ HO space. Because of the degeneracy of the l configurations in the $\Delta\mathcal{N} = 0$ HO space, a given state $|Nn_z\Lambda\rangle = \sum_l a_{Nl}^{n_z\Lambda}|Nl\Lambda\rangle$ is not dominated by a single configuration $|Nl\Lambda\rangle$, but involves contributions of all orbits with comparable amplitudes $a_{Nl}^{n_z\Lambda}$. The resulting $M1$ transition amplitude does not get its main contribution from the orbits with largest angular momentum, as in our case, but is an algebraic weighted sum of different contributions (with small weights) from all configurations, with both large and small l values, hence the enhanced $M1$ strength produced by our calculations.

The main results of our RPA calculation are (i) the $M1$ strength, at least in heavy clusters, is not concentrated only at low energy, as predicted by the schematic model, but spreads over a large energy region among equally spaced peaks corresponding to $\Delta\mathcal{N} = 0, 2, 4 \ldots,$ p-h transitions. (ii) In spite of that, closely packed $M1$ transitions still fall at low energy and carry an overall strength which is comparable to the value predicted in the schematic collective model. Such a strength can become huge in heavy clusters. It can reach the impressive value of $(350–400)\mu_b^2$ already at $N_e \sim 300$. (iii) The energy centroid of these transitions scales with the deformation and the number of valence electrons as in the schematic model only in heavy clusters. In the light ones, the strong fluctuations of the summed $M1$ strength invalidate the schematic model. (iv) The crucial role of the quadrupole field in promoting the $M1$ mode is confirmed by the close correlation established quantitatively between $M1$ and $E2$ modes. While however the $E2$ strength is concentrated mostly in the uninteresting region covered by the plasmon dipole resonance, the $M1$ is the only dominant mode at low energy with a strength which becomes huge in heavy clusters. These properties render the mode accessible to experiments. Its occurrence not only would indicate the onset of deformation but would enable one to measure the deformation itself by exploiting the scaling properties of the centroids with deformation and with the sizes of the clusters.

[1] E. Lipparini and S. Stringari, Phys. Rev. Lett. **63**, 570 (1989); Z. Phys. D **18**, 193 (1991).
[2] N. Lo Iudice and F. Palumbo, Phys. Rev. Lett. **41**, 1532 (1978).
[3] D. Bohle *et al.*, Phys. Lett. **137B**, 27 (1984).
[4] V. O. Nesterenko, W. Kleinig, V. V. Gudkov, N. Lo Iudice, and J. Kvasil, Phys. Rev. A **56**, 607 (1997).
[5] V. O. Nesterenko and W. Kleinig, in *Similarities and Differences between Atomic Nuclei and Clusters*, edited by Y. Abe, I. Arai, S. M. Lee, and K. Yabana, AIP Conf. Proc. No. 416 (AIP, New York, 1998), p. 77.
[6] W. Kleinig, V. O. Nesterenko, P.-G. Reinhard, and Ll. Serra, Eur. Phys. J. D **4**, 343 (1998).
[7] W. Kohn and L. J. Sham, Phys. Rev. **140**, A1133 (1965).
[8] N. Lo Iudice, Phys. Rev. C **57**, 1246 (1998).
[9] M. Schmidt and H. Haberland (private communication).
[10] S. Frauendorf and V. V. Pashkevich, Ann. Phys. (Leipzig) **5**, 34 (1996).
[11] K. Clemenger, Phys. Rev. B **32**, 1359 (1985).